A Tropical Cyclone Genesis Parameter for the Tropical Atlantic

MARK DeMARIA

NESDIS/ORA, Fort Collins, Colorado

JOHN A. KNAFF AND BERNADETTE H. CONNELL

Cooperative Institute for Research in the Atmosphere, Colorado State University, Fort Collins, Colorado

ABSTRACT

A parameter to evaluate the potential for tropical cyclone formation (genesis) in the North Atlantic between Africa and the Caribbean islands is developed. Climatologically, this region is the source of about 40% of the Atlantic basin tropical cyclones but roughly 60% of the major hurricanes. The genesis parameter is the product of appropriately scaled 5-day running mean vertical shear, vertical instability, and midlevel moisture variables. The instability and shear variables are calculated from operational NCEP analyses, and the midlevel moisture variable is determined from cloud-cleared GOES water vapor imagery. The average shear and instability variables from 1991 to 1999 and moisture variable from 1995 to 1999 indicate that tropical cyclone formation in the early part of the season is limited by the vertical instability and midlevel moisture. Formation at the end of the season is limited by the vertical shear. On average, there is only a short period from mid-July to mid-October when all three variables are favorable for development. This observation helps explains why tropical cyclone formation in the tropical Atlantic has such a peaked distribution in time. The parameter also helps explain intra- and interseasonal variability in tropical cyclone formation. An independent evaluation of the parameter and possible applications to operational forecasting are presented using data from the 2000 hurricane season. The possibility of determining additional thermodynamic information from the GOES sounder is also discussed.

1. Introduction

Although the Atlantic hurricane season extends from 1 June to 30 November, the majority of the tropical cyclones occur from mid-August to mid-October with a peak near 10 September (e.g., Neumann 1993). It is during this period when storms typically form from tropical waves in the Atlantic between the African coast and the Caribbean Islands. Figure 1 shows smoothed distributions of tropical cyclone formations from the beginning of the operational satellite era to the present (1966–99) as determined from the National Hurricane Center (NHC) best track. The date that genesis occurred was defined by the time when a named storm first became a tropical depression. Figure 1 shows that the distributions for the entire Atlantic basin and the tropical Atlantic (defined as the region from Africa to 60°W and south of 20°N) are very peaked in time. The distribution maximum occurs on 3 September for the Atlantic basin and on 29 August for the tropical Atlantic.

The annual variability in tropical cyclone genesis in the Atlantic and other tropical cyclone basins has been attributed to both thermodynamic and dynamical factors. Palmen (1948) indicated that a sea surface temperature (SST) of about 26°C is necessary for tropical cyclone formation. In a study of west Pacific typhoons, Riehl (1948) indicated that storm formation can be inhibited by the vertical shear of the horizontal wind. Gray (1968) defined a tropical cyclone genesis parameter as the product of thermodynamic and dynamical terms, where SST and midlevel moisture effects were included in the thermodynamic term, and vertical shear and low-level vorticity effects were included in the dynamical term. Climatological values of this parameter are well correlated with the global tropical cyclone formation regions (McBride 1995).

Further evidence of the effect of vertical shear on Atlantic tropical cyclone genesis is provided by studies of interannual variability of tropical cyclone activity, and its connection with the El Niño–Southern Oscillation (ENSO) phenomenon (e.g., Gray 1984). For example, in a comprehensive statistical study, Goldenberg and Shapiro (1996) have shown that the relationship between Atlantic major hurricane activity and ENSO is due to variations of vertical wind shear in the main development region (an area slightly larger than defined

Corresponding author address: Mark DeMaria, NOAA/NESDIS/ORA, Colorado State University, West Laporte Avenue, Fort Collins, CO 80523.
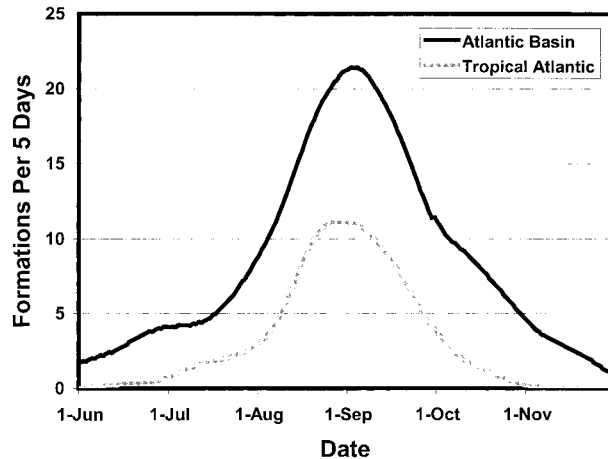E-mail: demaria@cira.colostate.edu

FIG. 1. Smoothed distributions of the number of tropical cyclone formations per 5 days in the Atlantic basin and the tropical Atlantic (0°–20°N, 0°–60°W). The distributions are based upon the National Hurricane Center best track data from 1966 to 1999.

FIG. 2. The formation locations of all named Atlantic tropical cyclones for the period 1966–99.

above as the tropical Atlantic), which arise from Walker circulation variations in response to the equatorial Pacific SST and convective anomalies. The studies of interannual variability have also suggested a direct relationship between Atlantic SST variations and Atlantic storms. Shapiro and Goldenberg (1998) have shown that when the tropical Atlantic SSTs are higher than normal, there tends to be increased numbers of tropical cyclones. Landsea et al. (1999) also show the strong modulating effect of Atlantic SST upon tropical cyclone activity, especially those forming in the Tropics.

Despite the well-documented relationships between the prestorm environment and tropical cyclone genesis described above, the prediction of whether or not an individual tropical disturbance will become a tropical storm remains a very difficult task. Recently, global forecast models have shown some ability in predicting tropical cyclone formation. However, the false alarm rate in global models can sometimes be large. For example, an informal study of tropical cyclone genesis in the National Centers for Environmental Prediction (NCEP) global model was performed for the 1996 Atlantic hurricane season. It was found that observed tropical cyclone genesis corresponded with areas in the model where the 700-hPa relative vorticity exceeded 4×10^{-5} s^{-1} and a closed circulation appeared at 1000 hPa. Using these criteria, the NCEP model correctly forecast the formation of 85%, 62%, and 29% of the 13 Atlantic storms during the 1996 season at lead times of 24, 48, and 72 h, respectively. However, using these same criteria, there were 14, 14, and 21 false alarms at 24, 48, and 72 h, respectively.

In this study, a genesis parameter for forecasting tropical cyclone formation in the tropical Atlantic is described. As will be described in section 2, this study is restricted to the tropical Atlantic because this region is the source for most of the major hurricanes in the At-
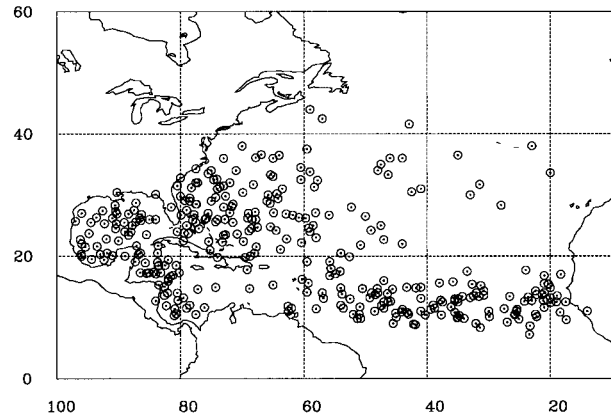
lantic basin, and because preexisting disturbances move through this area fairly regularly. The parameter includes thermodynamic and dynamical effects, and is calculated from operational global model analyses and Geostationary Operational Environmental Satellite (GOES) imagery. The genesis parameter is described in section 2. A climatology of the parameter and its relationship with the observed distribution of Atlantic storm formation is presented in section 3. In section 4, the variations in the parameter during 1991–99 and an independent evaluation during 2000, are described. In section 5, the possibility of generalizing the parameter using GOES sounder data is discussed.

2. The genesis parameter

Figure 2 shows the formation locations of all of the named Atlantic tropical cyclones from 1966 to 1999, as indicated by the first positions in the NHC best track. This study will be restricted to the region from Africa to 60°W, and south of 20°N (referred to as the tropical Atlantic). For the period 1966–99, this region was the source of 37% of the Atlantic basin tropical cyclones but 61% of the storms that eventually became major hurricanes.

The genesis parameter will only measure the large-scale environment. Many studies have shown that a preexisting disturbance is also required for tropical cyclone formation (e.g., Gray 1968; Emanuel 1989; Zehr 1992). About 60 tropical waves per year move across the Atlantic basin during the hurricane season (Frank and Clark 1980), so there is a fairly constant source of disturbances for tropical cyclone formation. To generalize this work to other regions, it would probably be necessary to include an indicator of whether a tropical disturbance was present. A generalization of this work might also include a measure of the intensity of the initial disturbance. For example, Molinari et al. (2000) suggested that because the environmental conditions in the eastern North Pacific tropical cyclone basin are near-

ly always favorable, the most important indicator of whether or not tropical cyclone genesis will occur is the amplitude of the tropical waves approaching this region.

It is interesting to note in Fig. 2 that there is a high concentration of formations at low latitudes between Africa and the Caribbean Islands, but very few formations in the eastern Caribbean. Molinari et al. (1997) indicated that there is a region in the tropical Atlantic from Africa to about 50°W where the large-scale potential vorticity (PV) gradient reverses sign. In this region, the necessary condition for barotropic–baroclinic instability is satisfied, which can provide an energy source for tropical waves. However, as the waves move away from this energy source region, their amplitude gradually decreases due to frictional dissipation. If a tropical cyclone does not form from the wave by the time it reaches the eastern Caribbean, Fig. 2 indicates that it is not likely to do so until it reaches the western Caribbean. Molinari et al. (1997) also point out that there is a secondary region of PV gradient reversal in the western Caribbean.

Many studies have shown that tropical cyclones are more likely to form in regions with low vertical wind shear (e.g., McBride and Zehr 1981). The first variable included in the genesis parameter is the zonal component of the 200–850-hPa vertical shear, averaged from 8° to 18°N, and from 30° to 50°W. This domain was chosen because it surrounds the centroid of the tropical Atlantic genesis locations in Fig. 2 and covers a larger area than the tropical disturbances that have the potential to become depressions. The shear variable is defined so that it is positive when the winds became more westerly with height. Only the zonal component is considered because at the low latitudes of this study, the zonal shear is highly correlated with the magnitude of the total shear. For example, during the 1999 hurricane season, the correlation coefficient between the area-averaged zonal shear magnitude and the total shear magnitude was 0.98. By considering only the zonal component, it is possible to distinguish between easterly and westerly shear with a single variable. The zonal shear was calculated at 0000 and 1200 UTC from June to November for 1991–99 using the operational analyses from the aviation run of the NCEP Medium Range Forecast (MRF) Model (hereafter, the aviation analyses). The shear values were calculated for the period from 1991 to 1999 because the aviation model analyses were readily available in an archive maintained for development of the operational version of the NHC Statistical Hurricane Intensity Prediction Scheme (DeMaria and Kaplan 1999).

As described in the introduction, the relationship between the SST and tropical cyclone formation has been recognized for many years. Palmen (1948) explained the influence of SST on storm formation by considering the effect of an undilute air parcel lifted from the surface to the tropopause, and the extreme sensitivity of the difference between the parcel and environmental temperature to the surface properties. A similar approach is used to include thermodynamic effects in the genesis parameter. For this purpose, the surface temperature, relative humidity, and surface pressure from the aviation analyses were averaged over the same area as for the vertical shear. These values were used to define an air parcel, which was lifted dry adiabatically from the surface to saturation, and moist adiabatically to 200 hPa. The parcel calculations were performed using the thermodynamic formulation described by Ooyama (1990), but without the inclusion of the ice phase (for simplicity). Then, the pressure-weighted temperature difference between the parcel and the environment is calculated from 850 to 200 hPa. This variable is positive when the parcel is warmer than the environment, so it will be referred to as the instability parameter. The instability parameter is directly proportional to the convective available potential energy when the parcel is warmer than the environment between 850 and 200 hPa. However, this parameter can also be negative, which allows the measurement of the stability and the instability with a single variable.

The instability parameter ranged from about −4° to 3°C. When this parameter is positive, it is unlikely that the atmosphere is convectively unstable over such a large region of the tropical ocean (Xu and Emanuel 1989; Williams 1993). If entrainment and water-loading effects were included, the largest value of the instability parameter would be closer to zero. However, it is possible for the tropical atmosphere to be very stable, especially in regions of subsidence. Thus, the instability parameter can be considered a measure of how far the large-scale tropical atmosphere is from convective neutrality.

The third contribution to the genesis parameter is a midlevel moisture variable. Entrainment of environmental air in convection leads to a reduction or elimination of buoyancy. If the entrained air is dry, downdrafts can be enhanced, and the equivalent potential temperature at the surface reduced. Bister and Emanuel (1997) have hypothesized that the moistening in the lower to middle troposphere, and the subsequent reduction in entrainment effects, is an important precursor for tropical cyclone formation.

Because moisture is a difficult parameter to measure (especially in the region considered in this study, which does not have radiosonde coverage) the aviation analyses were not used for the midlevel moisture variable. Instead, the brightness temperatures from *GOES-8* 6.7-μm (also referred to as water vapor or channel 3) imagery were used to derive the moisture parameter. As described by Moody et al. (1999), the GOES water vapor imagery in cloud-free regions is sensitive to the relative humidity in the mid- to upper troposphere. Because we are attempting to measure the environment in which the disturbances are moving through, rather than the disturbances themselves, the imagery was cleared of deep clouds by eliminating all pixels with brightness temperatures colder than −35°C. This temperature

threshold was chosen because the weighting function for the channel 3 imagery in cloud-free regions peaks near 300 hPa (Velden et al. 1997). The 300-hPa temperature from a mean tropical sounding (Jordan 1958) is about −35°C. Thus, brightness temperatures colder than this threshold are likely due to cold cloud tops from deep convection.

The brightness temperatures of all pixels (except those identified as containing deep convection) were averaged over an area from 8° to 18°N, and from 35° to 55°W. It was necessary to shift the brightness temperature region 5° to the west of the shear and instability regions to reduce the limb effect of the satellite (the subpoint of *GOES-8* is 75°W). The *GOES-8* water vapor imagery was available for the entire hurricane season in an archive maintained by the Cooperative Institute for Research in the Atmosphere for the period 1996–99. Imagery for part of July and most of August and September of 1995 were also available.

To smooth the data, 5-day running means of each variable are calculated from the daily values at 0000 and 1200 UTC. The date of each data point is referenced by the end of each 5-day period. The ending date of the period is used because, in real time, the data would only be available up to the current day. For the remainder of this paper, the references to the shear, instability, and moisture variables are for the 5-day means, unless otherwise specified.

The basic idea of the genesis parameter is to apply linear transformations to the shear, instability, and mid-level moisture variables, so that the transformed variables are negative when conditions are unfavorable for development, are zero when conditions are marginal, and have a value of unity when conditions are most favorable. Two conditions are required to define the linear transformation for each variable. These conditions are determined from the values of the variables at the time each of the storms formed during the period 1991–99.

Table 1 lists the 45 tropical cyclones that formed in the tropical Atlantic from 1991 to 1999. Seven storms remained depressions, 13 attained tropical storm intensity, 9 become nonmajor hurricanes (category 1 or 2), and 16 became major hurricanes (category 3 or higher). The tracks and intensities for the seven storms that remained depressions are not included in the NHC best track. The data for these cases were obtained from the NHC operational best track and were included to increase the sample size.

Figure 3 shows a scatter diagram of the values of the zonal shear and instability variables at the formation times of the 45 tropical cyclones in the tropical Atlantic. The values of the shear and instability for each storm case are also listed in Table 1. All except 1 (Hurricane Lisa in 1998) of the 45 storms formed when the vertical shear variable was ≤25 kt. Thus, the scaling is chosen so that the transformed shear parameter will become negative when the zonal shear exceeds 25 kt. To deter-

mine the second condition for the linear transformation of the shear, it might be argued that the most favorable conditions occur when the shear is zero. However, during the hurricane season, the tropical Atlantic makes a transition from westerly to easterly shear, and then back to westerly shear. From this point of view, the most favorable conditions occur when the tropical Atlantic is as far removed from the upper-level westerlies as possible, which occurs when the zonal shear is easterly. In addition, Tuleya and Kurihara (1981) performed idealized modeling studies of tropical cyclone genesis in environments with easterly, zero, and westerly vertical shear. Their results showed that when the low-level flow was from the east (similar to the tropical Atlantic), an environment with easterly vertical shear was more favorable for tropical cyclone genesis than a zero shear environment, and much more favorable than an environment with westerly shear. Thus, for the second condition for the transformation, the most favorable shear is considered to be −15 kt, which is close to the minimum observed value in Table 1 and Fig. 3.

With the above two conditions, the linearly transformed shear (*S*) is given by

$$S = (25 - S')/40, \qquad (2.1)$$

where S' is the unscaled shear. The above equation shows that $S = 1$ when $S' = -15$ kt, and $S < 0$ when $S' > 25$ kt. In a few cases during the season, *S* was slightly greater than one, which occurs when $S' < -15$ kt. In these cases *S* was set equal to one.

To determine the linear transformation for the instability variable, Table 1 and Fig. 3 show that all but two storms [Tropical Depression (TD) 4 in 1991 and Hurricane Emily in 1993] formed when the instability variable was ≥ 0°C. In these cases the instability variable became positive within 1 (TD 4) or 2 (Emily) days. Thus, the scaling is chosen so that the transformed instability parameter is negative when the instability is negative. The maximum instability at the time of storm formation was ∼2.5°C. For the second condition for the transformation, it is assumed that 2.5°C is the most favorable value of the instability variable.

With the above two conditions, the linearly transformed instability parameter (*I*) is given by

$$I = I'/2.5, \qquad (2.2)$$

where I' is the unscaled instability parameter. Similar to *S*, the values of *I* were slightly greater than one in a few cases, but were set equal to one.

A similar scaling procedure was applied to the moisture variable. Five-day running means of the cloud-cleared area-averaged water vapor brightness temperatures were calculated for all available time periods from 1995 to 1999. Table 1 shows that mean brightness temperatures were available for 26 of the tropical Atlantic formations (these eventually became 3 unnamed depressions, 3 tropical storms, 9 nonmajor hurricanes, and 11 major hurricanes). In all except one case (Hurricane

TABLE 1. The 45 tropical cyclones that formed in the tropical Atlantic (0°–20°N, 0°–60°W) during the period 1991–99. The date, latitude, longitude, shear (S'), instability (I'), and moisture (M') variables at the time of formation, and the maximum intensity (kt) reached at any time during the storm life cycle are also listed. Asterisk (*) indicates missing data.

TD04	24 Aug 1991	14.5	23.1	1	−0.3	*	30
TD05	28 Aug 1991	10.5	30.8	2	0.9	*	30
Danny	7 Sep 1991	10.4	25.8	4	1.1	*	45
TD10	24 Oct 1991	13.4	42.3	21	1.2	*	25
Andrew	16 Aug 1992	10.8	35.5	−3	0.5	*	135
Bret	4 Aug 1993	10.4	40.3	0	1.2	*	50
Cindy	14 Aug 1993	14.1	59.5	−1	0.1	*	40
Dennis	23 Aug 1993	13.6	30.8	−5	0.0	*	45
Emily	22 Aug 1993	19.9	52.6	−4	−0.2	*	100
Chris	16 Aug 1994	11.3	39.4	−10	0.4	*	70
Debby	9 Sep 1994	13.1	56.8	1	0.3	*	60
Ernesto	21 Sep 1994	10.1	29.9	20	0.7	*	50
TD09	27 Sep 1994	13.8	20.8	19	0.4	*	30
Chantal	12 Jul 1995	17.1	54.9	3	0.9	*	60
Felix	8 Aug 1995	14.3	30.8	−9	1.6	*	120
Humberto	22 Aug 1995	13.2	33.0	−7	1.9	−27.8	95
Iris	22 Aug 1995	13.2	49.3	−7	1.9	−27.8	95
Karen	26 Aug 1995	15.4	32.7	−10	1.7	*	45
Luis	28 Aug 1995	11.4	27.5	−17	1.7	*	130
TD14	9 Sep 1995	17.9	41.9	1	1.9	−31.3	30
Marilyn	12 Sep 1995	11.7	50.9	−4	1.8	−29.5	100
Noel	26 Sep 1995	10.4	37.7	7	1.4	−29.8	65
Pablo	4 Oct 1995	8.3	31.4	20	1.5	*	50
Sebastien	20 Oct 1995	13.8	53.8	25	1.8	*	55
Bertha	5 Jul 1996	9.8	34.0	10	0.6	−27.5	100
Edouard	19 Aug 1996	12.4	19.9	−2	1.1	−27.4	125
Fran	23 Aug 1996	14.0	21.0	−4	1.6	−25.9	105
Gustav	26 Aug 1996	12.7	23.0	−8	2.1	−26.8	40
Hortense	3 Sep 1996	14.9	41.0	7	2.2	−31.6	120
Isidore	24 Sep 1996	8.6	23.3	22	1.6	−28.4	100
TD05	17 Jul 1997	12.0	51.5	7	0.8	−26.3	30
Erika	3 Sep 1997	10.9	44.1	7	1.8	−28.3	110
Alex	27 Jul 1998	11.3	25.4	1	1.0	−26.3	45
Bonnie	19 Aug 1998	14.7	48.1	−5	1.4	−26.3	100
Danielle	24 Aug 1998	13.4	34.3	−2	1.3	−29.4	90
Georges	15 Sep 1998	9.7	25.1	−5	1.8	−26.9	135
Ivan	19 Sep 1998	13.4	26.6	−6	1.7	−27.7	80
Jeanne	21 Sep 1998	9.6	17.4	2	1.7	−26.7	90
Lisa	5 Oct 1998	13.9	46.4	29	1.8	−29.0	65
Cindy	19 Aug 1999	13.5	18.9	−8	1.8	−26.6	120
Emily	24 Aug 1999	11.5	53.6	−18	2.2	−28.4	45
Floyd	7 Sep 1999	14.6	45.6	2	2.6	−28.5	135
Gert	11 Sep 1999	12.6	24.2	3	2.1	−28.2	130
TD12	6 Oct 1999	14.4	44.8	8	2.5	−28.2	30
Jose	17 Oct 1999	9.8	50.8	19	2.7	−31.0	85

Fran in 1996) the average brightness temperature was colder than −26.0°C at the formation time. However, Fran formed very far to the east, and the brightness temperature decreased below −26.0°C by the time the storm reached the area included in the brightness temperature calculation. Thus, the linearly transformed moisture variable is defined so that it becomes negative for brightness temperatures warmer than −26.0°C. The minimum brightness temperature value at the formation time was −31.6°C, although in most cases, the value was warmer than −31°C. Thus, the most favorable brightness temperature is considered to be −31°C.

Using the above thresholds, the linearly tranformed moisture variable (M) is given by

$$M = (−26.0 − M')/5.0, \qquad (2.3)$$

where M' is the unscaled average brightness temperature. Similar to the scaled shear and instability variables, M has a value of zero when conditions are marginal, a value of one when conditions are most favorable, and is negative when conditions are unfavorable. Similar to S and I, the value of M was set equal to one in the few cases when it exceeded one.

The scaled shear, instability, and moisture variables are used to define the genesis parameter under the assumption that if any one of the variables are unfavorable, then tropical cyclone formation is unlikely. With this assumption, the genesis parameter (GP) is defined as

$$\mathrm{GP} = \begin{cases} 100 \times S \times I \times M & \text{if } S > 0, \quad I > 0, \quad \text{and} \quad M > 0 \\ 0 & \text{if } S < 0, \quad I < 0, \quad \text{or} \quad M < 0. \end{cases} \qquad (2.4)$$

From (2.4) it can be seen that GP ranges from 0 to 100. The scaling factor in (2.4) is arbitrary, but a value of 100 was used to provide a reasonable range of variability for plotting purposes.

3. Genesis parameter climatology

As a first evaluation of the genesis parameter, (2.4) was evaluated using the climatological values of *S, I,* and *M* (1991–99 for *S* and *I,* and 1995–99 for *M*). Because the number of years used to calculate the average daily time series was fairly small, it was necessary to further smooth *S, I,* and *M* to highlight the seasonal cycle. For this purpose, the low-pass filter described by Shapiro (1975) was applied. This filter is a simple three-point running average with weights of 0.25, 0.5, and 0.25, and is sometimes referred to as a three-point binomial filter (Panofsky and Brier 1968). Successive applications of this filter can provide additional smoothing. Figure 4 shows the response function for 1, 20, 40, . . . , 100 applications of the filter on daily data. Figure 5 shows the effect of the filter on the distribution of tropical cyclone formation for the tropical Atlantic for the period 1966–99. For each day, the number of storms that formed within ±2 days are summed from the best track data. Because of the fairly short period of the record, the resulting time series contains considerable noise, in addition to the seasonal cycle. Figure 5 shows that the noise is damped after 100 applications of the binomial filter, but the seasonal cycle is retained. Both distributions shown in Fig. 1 were smoothed using this procedure. The time series of S and I used to calculate the climatological genesis parameter were smoothed using 30 applications of the filter, and the time series of *M* was smoothed using 90 applications. The number of filter applications for *S, I,* and *M* were chosen subjectively as the minimum number necessary to provide reasonably smooth time series. The binomial filter was applied to the climatological times series of *S, I,* and *M,* but was not applied to the time series of *S, I,* and *M* for each individual year described in the next section.

Figure 6 shows the climatological genesis parameter and the smoothed tropical Atlantic genesis distribution. As described previously, the amplitude of the genesis parameter is arbitrary and was chosen so that GP would range between 0 and 100. The two time series in Fig. 6 are highly correlated (the correlation coefficient is 0.97), and the distribution peaks are separated by only 4 days. The tails of the observed genesis distribution are somewhat wider than that of the genesis parameter. This might be expected, since very early or late storms probably occur during periods when the environmental

conditions in the tropical Atlantic deviate from the climatological conditions, but the genesis parameter was calculated from mean values of *S, I,* and *M.*

Figure 7 shows the 1991–99 average time series of *S* and *I,* and the 1995–99 average time series of *M.* As described previously, the thresholds for when the scaled values of *S, I,* and *M* become positive (favorable) are when the unscaled values are <25 kt, >0°C, and <−26°C, respectively. The zonal shear in Fig. 7 is large at the beginning of the hurricane season and becomes favorable by 24 June. The shear is most favorable in late August, and then becomes unfavorable by 12 October. The scaled instability (*I*) in Fig. 7 is negative until 8 July. After that time, it increases fairly steadily until early October, when it decreases slightly. However, it remains positive throughout November.

The scaled shear and stability variables in Fig. 7 show that the zonal shear variable becomes favorable before the instability variable. Thus, the start of the hurricane season in the tropical Atlantic appears to be limited by thermodynamic effects. However, the zonal shear variable becomes unfavorable much sooner than the instability variable, which indicates that the end of the tropical Atlantic season is determined by dynamical effects. The peaked tropical Atlantic genesis distribution can then be explained by the relatively short period of time when both the dynamical and thermodynamic variables are favorable.

The scaled midlevel moisture (*M*) in Fig. 7 is always positive. However, it reaches a minimum in mid-July and remains near its minimum value until about the third week in August, when it increases rapidly. This parameter helps explain why genesis in the tropical Atlantic is relatively rare in July, even though the shear and instability variables have already become favorable by the first week in July. It appears that from early July to mid-August, the upper-level relative humidity is lower than during the rest of the hurricane season. A possible explanation for this observation is that there is increased subsidence during this period, possibly due to circulations related to heating over the surrounding continental regions. This effect helps to further increase the steepness of the genesis parameter time series.

4. Genesis parameter during individual years

In the previous section it was shown that the genesis parameter calculated from climatological variables correlated well with the average seasonal distribution of tropical cyclone formation. In this section, the values of *S, I,* and *M,* and the resulting times series of GP, are presented for individual years from 1991 to 1999. As
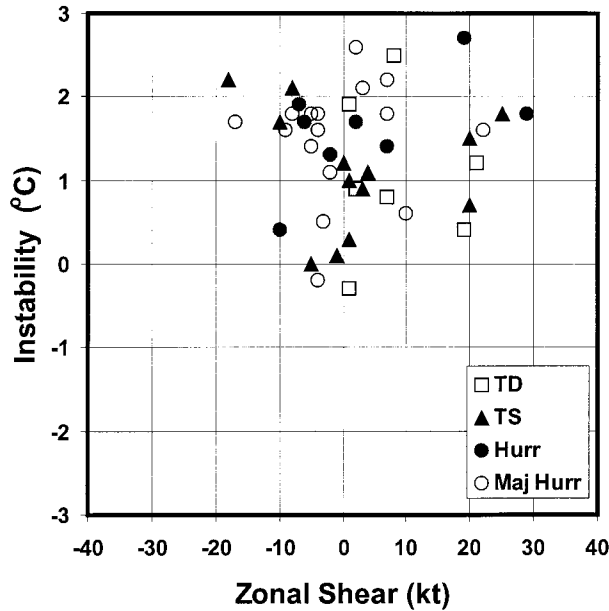
FIG. 3. A scatter diagram of the 5-day running mean zonal shear vs instability at the time of formation of the 45 tropical Atlantic tropical cyclones during the period 1991–99. The symbol type represents the maximum intensity reached at any point during the subsequent storm life cycle.

described in section 2, the *GOES-8* data for the complete hurricane season was only available beginning in 1996, with some data available for 1995 (mostly Aug and Sep). For the time periods without *GOES-8* data, the climatological value of *M* (shown in Fig. 7) was used to calculate GP. In a few cases, the NCEP aviation analyses were also not available (the first few days of Jun in 1991–95, and the last part of Nov 1995). For these periods, the values of *S* and *I* were set to zero. These short periods of missing NCEP analyses have little effect on the results described in this section, since they are
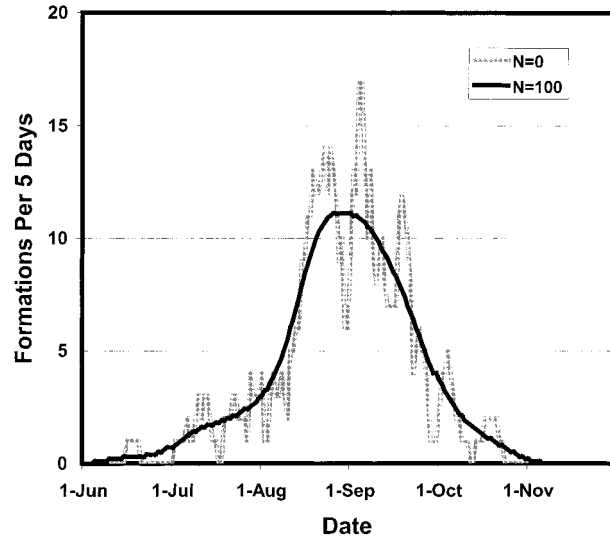

FIG. 5. The distribution of tropical Atlantic tropical cyclone formation before and after application of the binomial filter.

well before or after the period when genesis normally occurs in the tropical Atlantic.

Figure 8 shows the time series of *S, I,* and GP for 1991–93. [For display purposes, the GP in Fig. 8 (and also Figs. 9 and 10) was scaled to values between 0 and 2, rather than 0 to 100.] The climatological values of these variables and *M* are also shown in Fig. 8. The symbols just below the $y = 0$ line in the right panels of Fig. 8 indicate the times of tropical cyclone genesis, where the type of symbol denotes the maximum intensity reached by the storm (depression, tropical storm, hurricane, or major hurricane). Although long-term statistics for unnamed depressions were not available, during the period 1966–99, an average of 3.5 named storms formed per year, where an average of 1.4, 0.9, and 1.2 of these storms reached tropical storm, nonmajor hurricane, and major hurricane intensity, respectively.

FIG. 4. The response function for 1, 20, 40, . . . , 100 applications of the binomial filter as a function of period, for daily time series data.
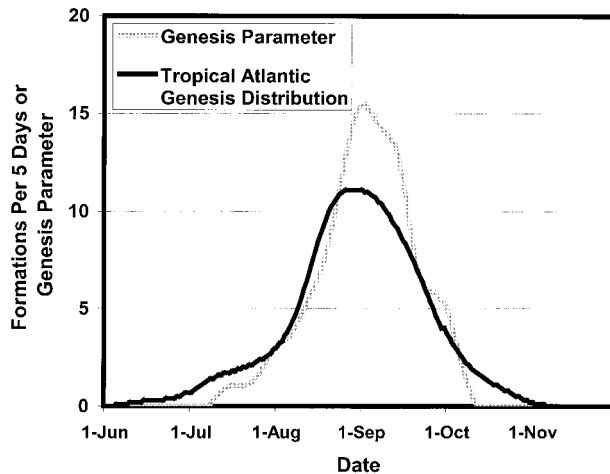

FIG. 6. The genesis parameter determined from climatological input and the smoothed tropical Atlantic genesis distribution.
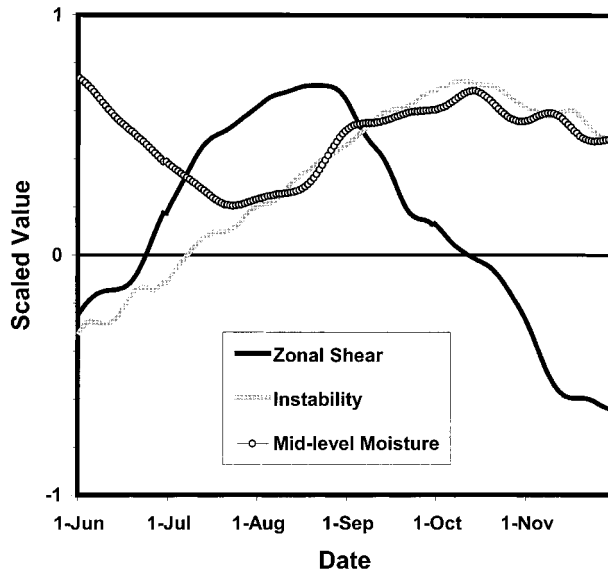
FIG. 7. Climatological time series of the scaled shear, instability, and moisture variables.

The time series for 1991 in Fig. 8 show that the GP was below average for nearly the entire hurricane season, and GP was positive for only a very short period. In the first part of the season, the low values of GP were primarily due to below normal instability. During September, the vertical shear parameter was lower than normal (indicating higher shear), which also contributed to the low values of GP. Although four tropical cyclones formed in the tropical Atlantic during 1991, the strongest of these only reached tropical storm strength, and the other three remained unnamed depressions.

The GP was also below normal for most of 1992 and 1993, although it was a little above normal at the beginning of 1993. The below normal values of GP were primarily due to low values of I, with some contribution from S. The 1992 season was very quiet, with only one storm developing in the tropical Atlantic (although this system developed into a major hurricane, Andrew). The early part of the 1993 season was fairly active, with four tropical cyclones before September. However, no storms formed in the tropical Atlantic after 23 August in 1993.

Figure 9 shows the time series for 1994–96. During 1994, the GP was again below normal for most of the season. In this year, S was a little more favorable than normal, but the instability was below normal for nearly the entire season. There were three named tropical cyclones in the tropical Atlantic in 1994, which was slightly below the long-term average. The GP changed dramatically in 1995, where it was above normal for nearly the entire season. The 1995 season was extremely active, with 11 tropical cyclones in the tropical Atlantic. The time series of GP for 1995 is a little noisier than for the previous years, since the observed values of M were used for part of the year. The very high values of GP

were due to higher than normal values of I during most of the season, with some contribution from S during part of the season. In addition, the values of M were also favorable during most of the season when they were available (not shown).

The bottom two panels of Fig. 9 show the time series for 1996. This was the first year for which M was available for the entire season, and is included in the lower-right panel in Fig. 9. This figure shows that M has fairly regular oscillations, with periods of about 2 weeks. In most cases, the amplitudes of these oscillations are not large enough to make M negative during the hurricane season except during the generally dry period in most of July and early August described previously. The year 1996 was also a fairly active hurricane season, especially in terms of the number of major hurricanes (five in the tropical Atlantic). The GP was above normal for parts of the season, but not as much as in 1995. It is interesting to note that the GP became positive much earlier than normal in 1996, and a major hurricane (Bertha) developed in early July.

Figure 10 shows the time series for 1997–99. The GP was generally above or near normal during the first half of the 1997 hurricane season. However, GP was zero for the latter half of September, primarily due to unfavorable shear. A very strong El Niño began during this time period, and the low values of S (high shear) are probably due to strong upper-level westerlies associated with a Walker-type circulation. The years 1998 and 1999 were generally active years, and the GP was above normal for a large fraction of these seasons (especially 1999). An exception to the above normal values of GP occurred during 1998 for several days in early September. This was caused by unusually low values of M, which corresponded to drying and subsidence. All of the tropical cyclone activity during 1998 occurred on either side of this dry period. It is possible that these type of dry events might contribute to the clustering in time of tropical cyclone activity in generally favorable years.

The above results indicate that the GP can partially explain the interannual variability in tropical cyclone activity and, sometimes, the intraseasonal variability in years like 1998. To provide a quantification of the relationship between the GP and seasonal tropical cyclone activity, a simple correlation was performed between the seasonal average (Jun–Nov) of GP and the number of tropical Atlantic storms in each year. The 1999 season had the largest average GP value (11.9), and the 1991 season had the lowest value (1.1). The climatological GP distribution had a seasonal average value of 3.4. The correlation between the average GP and the number of storms per year explained 41% of the variance and was statistically significant at the 95% level. This result indicates that seasons with high values of GP tend to be more active.

The application to forecasting becomes more clear when the GP is interpreted as a measure of the proba-
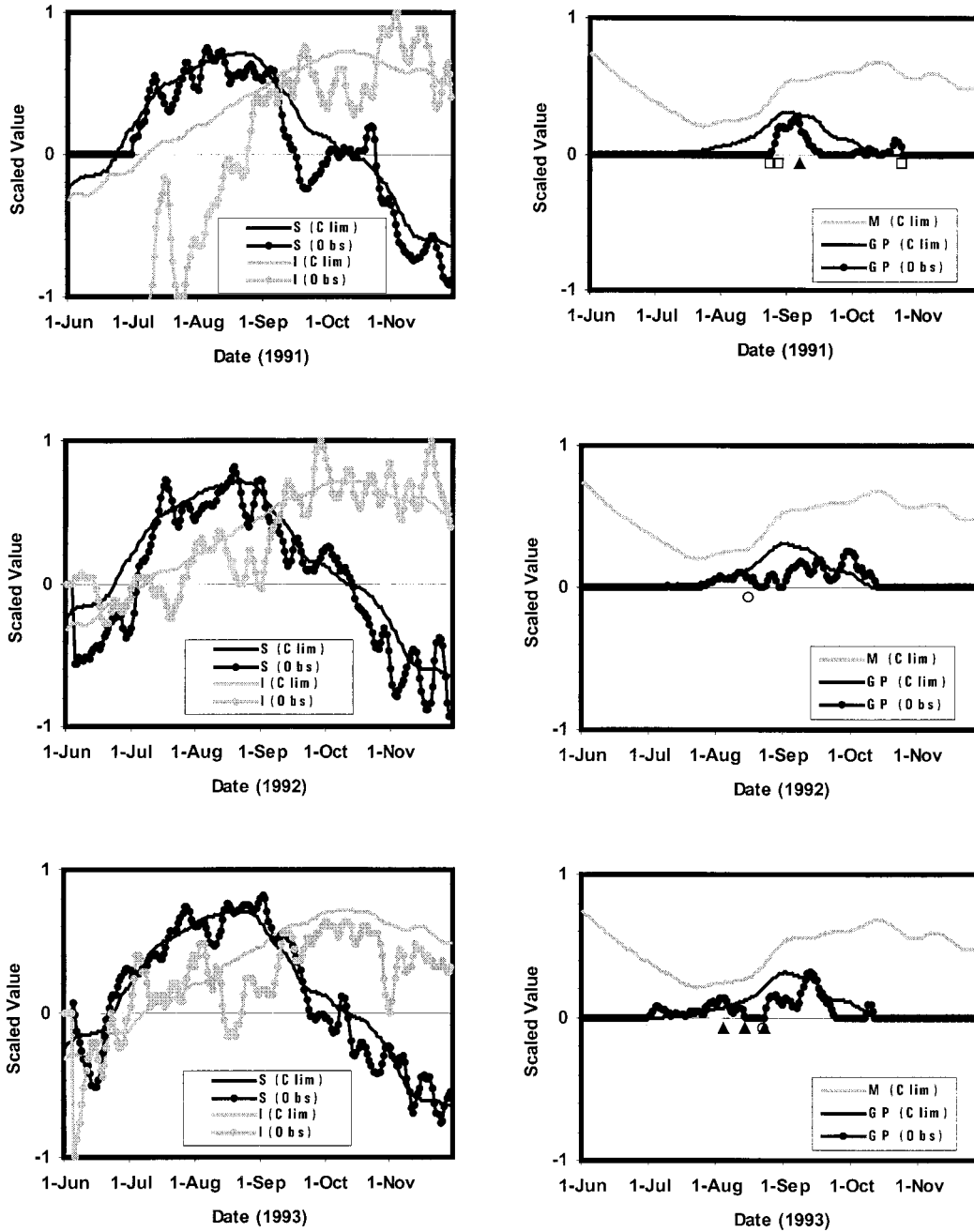
FIG. 8. Climatological and observed scaled shear, instability (left panels), moisture, and genesis parameter (right panels) for 1991–93. The symbols just below the $y = 0$ line (in the right-hand column) indicate the times of tropical cyclone formation during each year, where the type of symbol denotes the maximum intensity of the storm at any time during its life cycle (open square, closed triangle, closed circle, and open circle indicate depression, tropical storm, hurricane, and major hurricane, respectively).

bility of storm formation, relative to the climatological probability of formation. The climatological distribution of storm formation shown in Fig. 1 indicates that the probability for genesis in the tropical Atlantic during a day near the peak of the season is about 1 in 15 (11 formations per five days over the 34-yr period 1966–99). The close correspondence between the climatolog-

ical GP and the climatological genesis distribution in Fig. 6 indicates that the maximum probability of storm formation occurs when GP $\sim$ 15. As shown in Figs. 8–10, the daily GP values often have significant deviations from the climatological values. The sample of 45 storms from 1991 to 1999 is not large enough to completely map the probability distribution of formation as
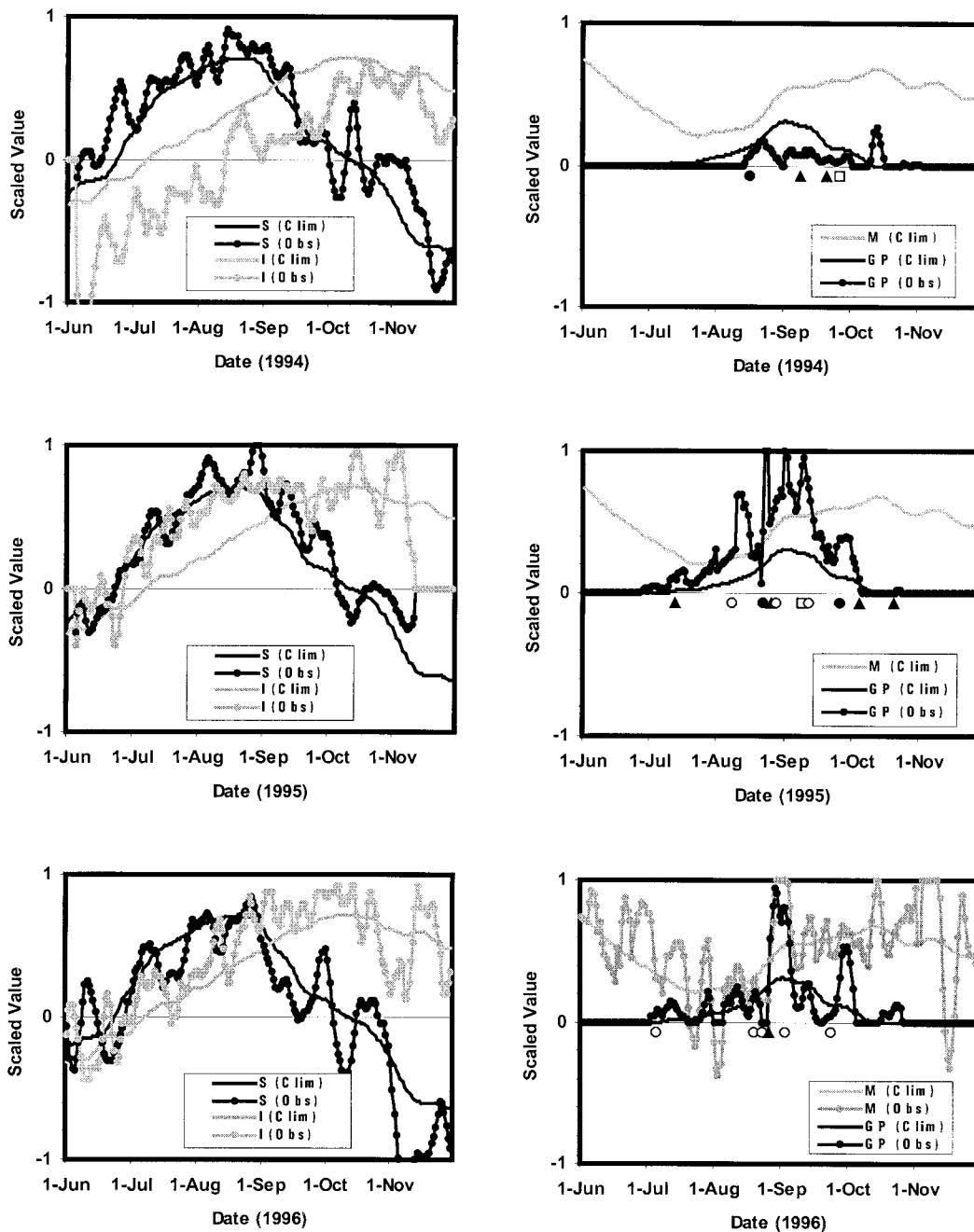
FIG. 9. Same as Fig. 8 but for 1994–96.

a function of the daily GP values. However, the GP at the time of formation for these 45 cases can be divided into three equal sized groups (15 cases each) as follows: 1) $0 \leq GP < 5$, 2) $5 \leq GP < 15$, 3) $15 \leq GP$. Based upon the distribution of the daily values of GP throughout the entire hurricane season from 1991 to 1999, the probability of formation for the three categories of GP is 74 to 1, 26 to 1, and 11 to 1. Thus, the larger the daily GP, the greater the probability of formation. The probability of genesis when the daily value of $GP > 15$

is about as large as the climatological probability of formation at the peak of the season.

To illustrate the operational use of GP, Fig. 11 shows the GP for the 2000 season, and that based upon the climatological values of *S, I,* and *M* from 1991–1999. This is a completely independent evaluation of GP since the 2000 cases were not used to determine the scaling for the transformed values of *S, I,* and *M.* The 2000 season was quite active with eight tropical cyclone formations in the tropical Atlantic, which eventually be-
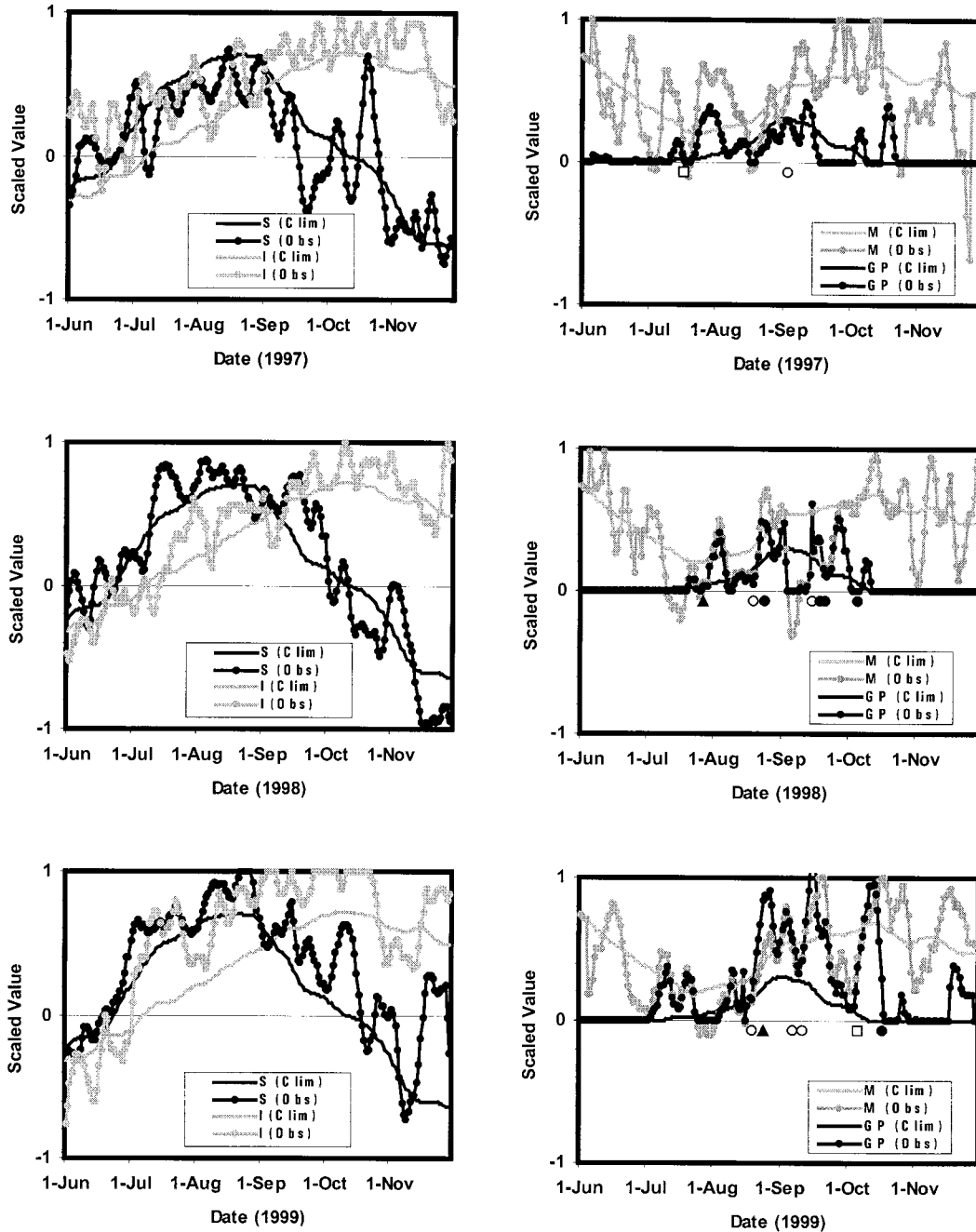
Fig. 10. Same as Fig. 8 but for 1997–99.

came a depression (TD02), three tropical storms (Chris, Ernesto, Helene), two hurricanes (Debby, Joyce), and two major hurricanes (Alberto, Isaac). The symbols along the 2000 GP curve in Fig. 11 indicate the times of formation of each of these storms, using the same convention for the symbols as in Figs. 8–10. TD02 was a very short-lived depression that formed very early in the season (24 Jun) and very far east (30°W). The GP was zero when TD02 formed, so it was not a good indicator for this case. In early August, the GP became

much larger than average. It exceeded 15 during 4–7 August, indicating that the probability of formation was as large or larger than during the peak of an average season. Alberto formed on 4 August and eventually became a major hurricane. The GP remained generally above average for most of August, and Alberto was followed by Tropical Storm Chris and Hurricane Debby. As the climatological peak of the season approached, the GP became much lower than average, and there was only one short-lived tropical storm (Ernesto) from 20
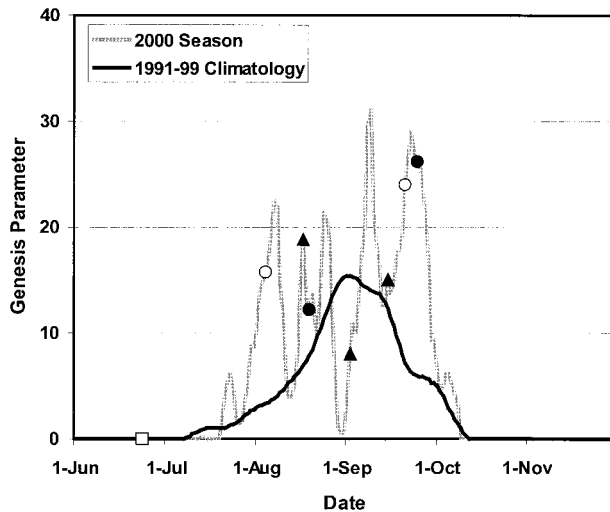
FIG. 11. The GP for the 2000 hurricane season and the GP calculated from climatological values of *S, I,* and *M.* The symbols along the 2000 season GP curve indicate the genesis times of the eight storms that formed in the tropical Atlantic. The type of symbol denotes the subsequent maximum intensity of the storm (open square, closed triangle, closed circle, and open circle indicate depression, tropical storm, hurricane, and major hurricane, respectively).

FIG. 12. Location of the *GOES-8* east Caribbean sounder sector.

August to 14 September. Thus, the GP in late August indicated that the probability of genesis was very low, even though this is normally the most favorable time for development. The GP again became larger than normal from early September to early October, when Tropical Storm Helene, major Hurricane Isaac, and Hurricane Joyce formed. The GP became zero at about the same time as the climatological GP, and there were no more tropical cyclone formations in the tropical Atlantic after this time.

5. Inclusion of GOES sounder data

The thermodynamic information used in the creation of the genesis parameter could be improved by including information derived from the GOES atmospheric sounder instrument. The latest generation of the GOES satellite has separate instruments for performing imaging and sounding operations, eliminating the scheduling conflicts of the past while providing better sounding capabilities than its predecessor. The *GOES-8* sounder has 18 thermal infrared bands plus a low-resolution visible band. The field of view is 8 km and is sampled every 10 km; 13-bit data are transmitted. The *GOES-8* sounder spectral selection was patterned after the High-Resolution Infrared Radiation Sounder carried on the National Oceanic and Atmospheric Administration (NOAA) polar-orbiting satellite. It has six channels in the 15-μm (long wave) band, a split-window pair, three midtropospheric water-sensitive channels and an ozone channel (midwave), five 4-μm (short wave) channels, and a visible channel. The spectral bands are sensitive to temperature, moisture, and ozone. The fulltime avail-
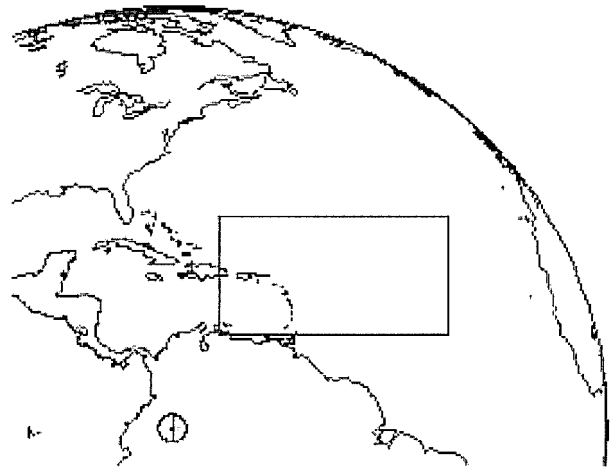
ability of the *GOES-8* sounder enables the creation of operational sounding products for the first time (Menzel and Purdom 1994). It is these sounder-based products that the genesis parameter may be able to exploit.

With the introduction of *GOES-8,* NOAA began making operational geostationary soundings. The soundings, which are created in clear field of view (FOV), include temperature and moisture profiles. Vertical temperature profiles from sounder radiance measurements are produced at 40 pressure levels from 1000 to 0.1 hPa using a physical retrieval algorithm that solves for surface skin temperature, atmospheric temperature, and atmospheric moisture simultaneously. The retrieval begins with a first-guess temperature profile that is obtained from a space–time interpolation of fields provided by NCEP forecast models. At this time the aviation run of the NCEP global model forecast is used to create the first guess. Hourly surface observations and SST from an Advanced Very High Resolution Radiometer help provide surface boundary information. Soundings are produced from 3 $\times$ 3 array FOVs whenever nine or more FOVs are determined to be either clear or contaminated only by "low cloud."

Vertical moisture (mixing ratio—hence, specific humidity) profiles are obtained in the simultaneous retrieval and are provided at the same levels as temperature up to 300 hPa. Since the radiance measurements respond to the total integrated moisture above a particular pressure level, the specific humidity is a differentiated quantity rather than an absolute retrieval. Layer means of either temperature or moisture can also be derived. Layered precipitable water can be integrated from retrievals of specific humidity; three layers (1000–900, 900–700, and 700–300 hPa) and the total atmospheric column precipitable water are provided as output products.

The GOES sounder products were used in a similar manner to the variables described previously to examine tropical cyclone genesis in the tropical Atlantic. Using the eastern Caribbean sounding sector (Fig. 12) in an
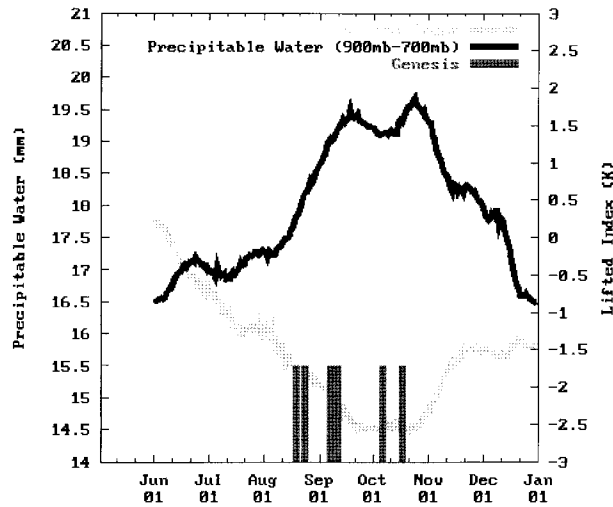
FIG. 13. Time series of the lifted index and 900–700-hPa precipitable water derived from the *GOES-8* sounder products. Note that a 5-day running mean has been applied to both series.
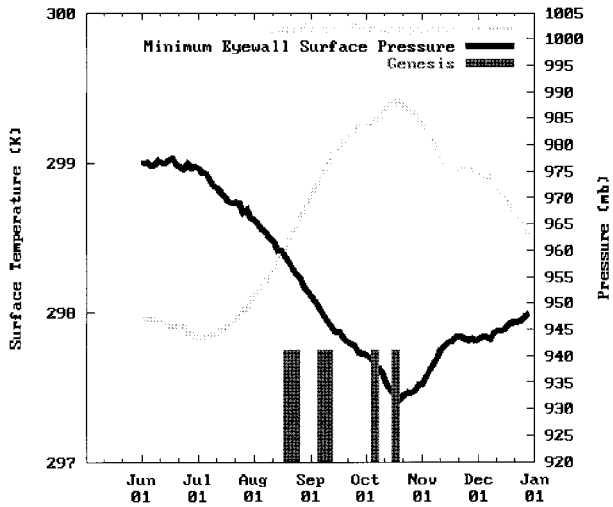

FIG. 14. Same as Fig. 13 except for area-average surface temperature and minimum eyewall pressure.

area between 40° and 50°W and 10° and 18°N, average vertical profiles of temperature and moisture are created. These area-averaged soundings are then used to derive several quantities thought useful for tropical cyclone genesis. They include the following.

Lifted Indices (LI): The Lifted Index is calculated by lifting a parcel of air dry adiabatically while conserving moisture until it reaches saturation. At that point the parcel is lifted moist adiabatically up to 500 hPa. If the parcel is warmer than the environment (i.e., negative LI), it has positive buoyancy and will tend to continue to rise. This parameter is somewhat similar to the instability parameter described previously.

Precipitable water (PW): An integrated measure of the atmospheric water content available in a vertical column, which in this case is derived from an areal average of GOES soundings. The PW can be measured throughout the depth of the atmosphere or in discrete layers. In the tropical atmosphere, where the environment is often conditionally unstable, the moisture content of the environment in which a cloud grows is often more important than the amount of environmental instability. As clouds grow they entrain environmental air and cool. Eventually this evaporative cooling will halt further cloud development. The amount of moisture in the lower layers of the atmosphere (900–700 hPa) is important to the evolution of cloud and cloud cluster–tropical cyclone development.

Maximum potential intensity (MPI): Following Holland (1997), an estimate of the maximum intensity a tropical cyclone may obtain (minimum eyewall pressure) can be derived from an environmental sounding (in this case an areal average from the GOES sounding). This is accomplished using an

iterative approach whereby the temperature of the environment is assumed to become the same as an undiluted rising parcel (which has a given surface temperature and pressure and is assumed to have a 90% relative humidity). The environmental warming that occurs during this process is integrated through the atmosphere resulting in a surface pressure decrease. At this point, a new parcel equivalent potential temperature is calculated and the process is repeated until convergence occurs (i.e., when the surface parcel is neutral and no further surface pressure decrease can be realized). Besides offering a measure of maximum potential intensity, the MPI parameter, given as eyewall surface pressure, is a direct measure of the absolute environmental instability.

Time series of these quantities seem well related to the genesis of tropical cyclones in the tropical Atlantic, and are consistent with the idea that the thermodynamics of the system determine the starting date. The time series of 1999 lifted index, 900–700-hPa precipitable water, and genesis times are shown together in Fig. 13. Using 1999 as an example, it might be expected that genesis will occur when the lifted index is less than −1.5°C and the precipitable water in the 900–700-hPa layer is greater than 17 mm. Sounder data from additional years will be necessary to confirm this hypothesis.

The surface temperature and minimum eyewall pressure are shown together in Fig. 14. In a similar manner, this plot indicates that genesis does not occur when the surface temperature in this area is less than 298.15 K (25°C), which is what would be expected based upon previous studies of SST thresholds for development (e.g., Palmen 1948). More interesting is the calculation of eyewall minimum pressure, which goes along with the surface temperature to some degree, and has a threshold value near 970 hPa. It is clear in Figs. 13 and

14 that for most of the season, these thresholds are met, suggesting again that the thermodynamics determine the beginning of the season. However, because these thermodynamic measures contain no information about the environmental winds, they too would need to be combined with some measure of vertical wind shear to better predict genesis. How to best combine sounder, model, and imager data is a subject for future research.

6. Concluding remarks

A parameter to evaluate the potential for tropical cyclone genesis in the North Atlantic between Africa and the Caribbean Islands was developed. Climatologically, this region is the source of about 40% of the Atlantic basin tropical cyclones but roughly 60% of the major hurricanes. The genesis parameter is the product of appropriately scaled 5-day running mean vertical shear, vertical instability, and midlevel moisture variables. The shear and instability variables were calculated from operational NCEP analyses, and the midlevel moisture variable was determined from cloud-cleared GOES water vapor imagery. The average shear and instability variables from 1991 to 1999 and moisture variable from 1995 to 1999 indicate that tropical cyclone formation in the early part of the season is limited by the vertical instability and midlevel moisture. Formation at the end of the season is limited by the vertical shear. On average, there is only a short period from mid-July to mid-October when all three variables are favorable for development. This observation helps explains why tropical cyclone formation in the tropical Atlantic has such a peaked distribution in time. The genesis parameter also helps explain intra- and interseasonal variability in tropical cyclone formation.

Time series indicated that in very active years the genesis parameter tended to be above normal and was positive for longer periods during the hurricane season. However, the time series also showed that the genesis parameter was positive for long periods without tropical cyclone formation. This result indicates that a positive value of the parameter represents a necessary condition for development, but is not a sufficient condition. However, as shown for the 2000 hurricane season, the parameter is useful for identifying periods with above and below normal probabilities of genesis.

This work could be generalized in a number of ways. The current version of the parameter only measures properties of the environment of a potential tropical cyclone. It might also be possible to determine the characteristics of the disturbance itself by measuring cloud-top temperatures from GOES imagery or low-level vorticity using large-scale analyses. In addition, the use of the GOES sounder data to provide more detailed thermodynamic information showed promise during the 1999 season. For example, the sounder data provides estimates of low-level moisture, which could be combined with the mid- to upper-level moisture parameter determined from the GOES channel 3 imagery. The sounder data from the 2000 season are being analyzed for comparison with the data from 1999.

Another limitation of this study is that the area where the genesis parameter was calculated was geographically fixed. This allowed the calculation of climatological statistics and interyear comparisons. It might also be possible to develop a disturbance-centered parameter, which could be used to evaluate individual systems. For example, Zehr (1992) showed that a genesis parameter was useful in differentiating between developing and nondeveloping tropical disturbances in the western North Pacific. His parameter was computed from objective analyses of 850-hPa relative vorticity and divergence, and 200–850-hPa vertical shear around tropical disturbances. Further research is necessary to evaluate the applicability of the simple thresholding technique to the disturbance-relative analysis, and to determine if some of the variables included in Zehr's parameter provide an adequate measure of the disturbance itself. Further study is also necessary to determine the applicability of this approach to other regions of the Atlantic basin, and to other tropical cyclone basins.

REFERENCES

Bister, M., and K. A. Emanuel, 1997: The genesis of Hurricane Guillermo: TEXMEX analyses and a modeling study. *Mon. Wea. Rev.,* **125,** 2662–2682.

DeMaria, M., and J. Kaplan, 1999: An updated Statistical Hurricane Intensity Prediction Scheme (SHIPS) for the Atlantic and eastern North Pacific basins. *Wea. Forecasting,* **14,** 326–337.

Emanuel, K. A., 1989: The finite amplitude nature of tropical cyclogenesis. *J. Atmos. Sci.,* **46,** 3431–3456.

Frank, N. L., and G. Clark, 1980: Atlantic tropical systems of 1979. *Mon. Wea. Rev.,* **108,** 966–972.

Goldenberg, S. B., and L. J. Shapiro, 1996: Physical mechanisms for the association of El Niño and west African rainfall with Atlantic major hurricane activity. *J. Climate,* **9,** 1169–1187.

Gray, W. M., 1968: Global view of the origin of tropical disturbances and storms. *Mon. Wea. Rev.,* **96,** 669–700.

——, 1984: Atlantic seasonal hurricane frequency. Part I: El Niño and 30 mb quasi-biennial oscillation influences. *Mon. Wea. Rev.,* **112,** 1649–1668.

Holland, G. J., 1997: The maximum potential intensity of tropical cyclones. *J. Atmos. Sci,* **54,** 2519–2541.

Jordan, C. L., 1958: Mean soundings for the West Indies area. *J. Meteor.,* **15,** 91–97.

Landsea, C. W., R. A. Pielke Jr., A. M. Mestas-Nunez, and J. A. Knaff, 1999: Atlantic basin hurricanes: Indices of climatic changes. *Climatic Change,* **42,** 89–129.

McBride, J. L., 1995: Tropical cyclone formation. *Global Perspectives on Tropical Cyclones,* WMO/TD No. 693, Rep. TCP-38, World Meteorological Organization, 63–105.

——, and R. M. Zehr, 1981: Observational analysis of tropical cyclone formation. Part II: Comparison of non-developing versus developing systems. *J. Atmos. Sci.,* **38,** 1132–1151.

Menzel, W. P., and J. F. W. Purdom, 1994: Introducing GOES-I: The
    first of a new generation of geostationary operational environ-
    mental satellites. *Bull. Amer. Meteor. Soc.,* **75,** 757–781.

Molinari, J., D. Knight, M. Dickinson, D. Vollaro, and S. Skubis,
    1997: Potential vorticity, easterly waves, and eastern Pacific
    tropical cyclogenesis. *Mon. Wea. Rev.,* **125,** 2699–2708.

——, D. Vollaro, S. Skubis, and M. Dickinson, 2000: Origins and
    mechanisms of eastern Pacific tropical cyclogenesis: A case
    study. *Mon. Wea. Rev.,* **128,** 125–139.

Moody, J. L., A. J. Wimmers, and J. C. Davenport, 1999: Remotely
    sensed specific humidity: Development of a derived product from
    the GOES Imager channel 3. *Geophys. Res. Lett.,* **26,** 59–62.

Neumann, C. J., 1993: Global climatology. *Global Guide to Tropical
    Cyclone Forecasting,* WMO/TD No. 560, Rep. TCP-31, World
    Meteorological Organization, 1.1–1.43.

Ooyama, K. V., 1990: A thermodynamic foundation for modeling the
    moist atmosphere. *J. Atmos. Sci.,* **47,** 2580–2593.

Palmen, E., 1948: On the formation and structure of tropical cyclones.
    Geophysics, **3,** 26–38.

Panofsky, H. A., and G. W. Brier, 1968: *Some Applications of Sta-
    tistics to Meteorology.* College of Earth and Mineral Sciences,
    The Pennsylvania State University, 224 pp.

Riehl, H., 1948: On the formation of typhoons. *J. Meteor.,* **5,** 247–
    264.

Shapiro, L. J., and S. B. Goldenberg, 1998: Atlantic sea surface
    temperatures and tropical cyclone formation. *J. Climate,* **11,**
    578–590.

Shapiro, R., 1975: Linear filtering. *Math. Comput.,* **29,** 1094–1097.

Tuleya, R. E., and Y. Kurihara, 1981: A numerical study on the effects
    of environmental flow on tropical storm genesis. *Mon. Wea. Rev.,*
    109, 2487–2506.

Velden, C. S., C. M. Hayden, S. J. Niemann, W. P. Menzel, S. Wan-
    zong, and J. S. Goerss, 1997: Winds derived from geostationary
    satellite moisture channel observations: Applications and impact
    on numerical weather prediction. *Bull. Amer. Meteor. Soc.,* **78,**
    173–195.

Williams, E., 1993: An analysis of the conditional instability of the
    tropical atmosphere. *Mon. Wea. Rev.,* **121,** 21–36.

Xu, K., and K. A. Emanuel, 1989: Is the tropical atmosphere con-
    ditionally unstable? *Mon. Wea. Rev.,* **117,** 1471–1479.

Zehr, R. M., 1992: Tropical cyclogenesis in the western north Pacific.
    NOAA Tech. Rep. NESDIS 61, 181 pp. [Available from NOAA/
    National Environmental Satellite, Data, and Information Service,
    Washington, DC 20233.]